

# Modeling of RC shear walls strengthened by FRP composites

Mohammed A. Sakr<sup>\*</sup>, Saher R. El-khoriby<sup>a</sup>, Tarek M. Khalifa<sup>b</sup> and Mohammed T. Nagib<sup>c</sup>

Department of Structural Engineering, Tanta University, Tanta, Egypt

(Received July 18, 2016, Revised November 13, 2016, Accepted December 16, 2016)

**Abstract.** RC shear walls are considered one of the main lateral resisting members in buildings. In recent years, FRP has been widely utilized in order to strengthen and retrofit concrete structures. A number of experimental studies used CFRP sheets as an external bracing system for retrofitting of RC shear walls. It has been found that the common mode of failure is the debonding of the CFRP-concrete adhesive material. In this study, behavior of RC shear wall was investigated with three different micro models. The analysis included 2D model using plane stress element, 3D model using shell element and 3D model using solid element. To allow for the debonding mode of failure, the adhesive layer was modeled using cohesive surface-to-surface interaction model at 3D analysis model and node-to-node interaction method using Cartesian elastic-plastic connector element at 2D analysis model. The FE model results are validated comparing the experimental results in the literature. It is shown that the proposed FE model can predict the modes of failure due to debonding of CFRP and behavior of CFRP strengthened RC shear wall reasonably well. Additionally, using 2D plane stress model, many parameters on the behavior of the cohesive surfaces are investigated such as fracture energy, interfacial shear stress, partial bonding, proposed CFRP anchor location and using different bracing of CFRP strips. Using two anchors near end of each diagonal CFRP strips delay the end debonding and increase the ductility for RC shear walls.

**Keywords:** finite element model; RC shear walls; cohesive interaction; CFRP; strengthening; debonding

## 1. Introduction

Reinforced concrete (RC) shear walls are the most common systems resisting lateral loads in concrete buildings. During an earthquake, the RC shear walls play a major role in limiting the seismic damage intensity by reducing the floor displacement for tall concrete buildings. Other advantages that make the RC shear walls a favourite lateral load resisting system are their construction simplicity and low cost. RC shear walls must be carefully designed to provide not only adequate strength, but also sufficient ductility to avoid brittle failure under strong lateral loads. Many RC shear walls all over the world are suffering damages from previous earthquakes or have poor detailing in design or have construction faults, and are in urgent need of rehabilitation. Fiber reinforced polymer (FRP) has been widely utilized in order to strengthen and retrofit concrete structures because of high strength-to-weight ratio, corrosion resistances, good fatigue characteristic and easy of handling. On the other hand, FRP materials suffer from disadvantages like low fire resistance, non-susceptibility to

bend in the field and high cost.

Many experimental works have been conducted to investigate the seismic behavior of RC shear walls strengthened with carbon fiber-reinforced polymer (CFRP) to predict the inelastic strength of walls subjected to lateral loading and to assess the natural frequencies of the walls such as Antoniadis *et al.* (2007), Dan (2012), El-Sokkary and Galal (2013), Qazi *et al.* (2013). The experimental results indicated that the CFRP strengthening technique adopted worked well with respect to improving specimen strength, reducing deformity and dissipating energy compared to the bare RC shear walls. Zhou *et al.* (2013) investigated experimentally the retrofitted of RC shear wall using a newly developed composite is being termed "CarbonFlex". This composite helped to stabilize the propagation of damage, specifically fracture, an energy dissipation mechanism, resulting in significant ductility and confinement and highstrength sustainability. Mohammed *et al.* (2013) investigated the significance of needing for an opening in the RC shear walls after the construction for doors, windows and essential services causes local cracking around the opening which leads to decrease in load carrying capacity. They have used CFRP for strengthening the openings. The panels were subjected to a uniformly distributed axial load with an eccentricity of  $t/6$ . The results showed that RC shear walls with openings strengthened by CFRP applied in  $45^\circ$  to the opening corners failed at load higher than failure load of their identical RC shear walls strengthened by CFRP applied along the opening. Altin *et al.* (2013) presented the behavior of RC shear walls strengthened with CFRP strips with different configurations of bracing under cyclic lateral loading. CFRP strips were

\*Corresponding author, Associate Professor  
E-mail: mhsakr010@yahoo.com

<sup>a</sup>Professor  
E-mail: saher.ibrahim@f-eng.tanta.edu.eg

<sup>b</sup>Lecturer Professor  
E-mail: tarek\_moh@yahoo.com

<sup>c</sup>Graduate Student  
E-mail: engm\_tolba@yahoo.com

controlled shear crack propagation and resulted in improvement of displacement capacity. Qazi *et al.* (2015) investigated the significance of partially bonding CFRP to RC shear walls under monotonic lateral loading. The strengthening arrangement consisted of partial bonding of CFRP strips to the wall panel and mesh anchors installation at the wall foundation joint. The reported test results showed that the adopted strengthening technique can improve wall performance in terms of strength and deformability with negligible variation in RC shear wall dissipation capacity.

Concurrently, finite element (FE) analysis has also been implemented, as a cost effective tool available to researcher all around the world, to predict the behavior of FRP strengthened RC shear walls. Li *et al.* (2005) used a non-linear 3-D FE analysis model using the FE analysis package (ABAQUS) to predict the cyclic behavior of RC shear wall structures. In this FE model, SPRING element is used to simulate the constraint deformation due to FRP wrapping, and improved concrete stress-strain curve is considered to account for the improvement of strength and ductility of concrete under FRP confinement. A damaged plasticity-based concrete model was used to capture the behavior of concrete under cyclic loading. Method to identify shear failure due to FRP debonding and FRP rupture in FE analysis is also proposed. The model was validated using the results from the experimental study. Mostofinejad and Anaei (2012) studied the effect of confining of boundary elements of slender RC shear wall by FRP composites and stirrups on flexural behavior of the wall under monotonic loading. The FE model was built using ABAQUS software. The interaction between the concrete and the FRP was modeled considering full bonding. Results of this study showed that the confinement of the boundary elements with FRP increased the ultimate displacement under almost constant load up to 50%. Furthermore, the results showed that it is sufficient to apply the FRP layers only on the boundary elements in the plastic hinge region of the wall. Cruz *et al.* (2012) presented the experimental results and preliminary analytical findings of a comprehensive study of RC shear walls repaired and strengthened using externally-bonded FRP two sheets. A FE program, VecTor2 was used to model the response of the RC shear walls. The concrete was modeled as an orthotropic material with smeared, rotating cracks. The CFRP sheets were represented by a series of discrete trusses made of a brittle material with zero compressive strength connected to the concrete through interface link elements. Computer simulations confirmed that the FRP system is also effective in eliminating the brittle shear mode of failure in walls with insufficient shear reinforcement and non-ductile details. Behfarnia and Sayah (2012) studied the effects of fiber reinforced plastic on the ultimate load capacity of RC shear walls with openings using ABAQUS software. The FRP is considered as a linear elastic material until failure and the interaction between the concrete and the FRP is modeled without considering debonding. Alsayed *et al.* (2014) presented experimentally and numerically the compression behavior of CFRP strengthened wall like rectangular RC column after shape modification. ANSYS program was employed for the numerical simulation of the test columns. The bond

between FRP and concrete was modeled using the tie break surface-to-surface contact definition of ANSYS. The quasi-static loading procedure was adopted by imposing vertical displacement variation through the top end of the column. The actual failure of the strengthened column was due to crushing of concrete and buckling of longitudinal rebars.

To the author's knowledge, although experimental studies in literature showed that the common mode of failure of such RC shear walls is the debonding of the CFRP, there is no previous numerical study for modeling the behavior of CFRP strengthened RC shear walls capable of simulating the debonding mode of failure. This paper deals with the monotonic behavior of RC shear walls with special highlighting of modeling the interaction between FRP sheets and concrete. Firstly, the FE models of RC shear walls under monotonic loading patterns were established using (ABAQUS) software. Element types, nonlinearity material constitutive models and contact models for CFRP and concrete were proposed. Based on the verified FE method, parametric analysis was established to investigate the performance of CFRP strengthened RC shear walls under monotonic loading.

## 2. Finite element models

(ABAQUS) software was used to model the bare RC shear wall and the CFRP strengthened RC shear wall. Brief descriptions of the constitutive models that are used in the model are described below.

### 2.1 Constitutive models

The "Concrete damage plasticity model" was used to model the concrete behavior. This model assumes that the main two failure modes are tensile cracking and compressive crushing (ABAQUS). The elastic parameters required to establish the tension stress-strain curve are elastic modulus,  $E_c$ , and tensile strength,  $f_{ct}$ . According to the ACI-318 (1999)  $E_c$  and  $f_{ct}$  were calculated. To specify the post-peak tension failure behavior of concrete the fracture energy method was used. For the uni-axial compression stress-strain curve of the concrete, the stress-strain relationship proposed by Saenz (1964) was used as reported in Hu and Schnobrich (1989). The steel was assumed to be bilinear elastic-plastic material identical in tension and compression. The CFRP material was considered as linear elastic isotropic until rupture.

### 2.2 Interface between CFRP strips and the RC shear wall surface

To represent the interface between CFRP strips and the RC shear wall surface, the model was constructed using cohesive interface by the traction separation law to allow for the debonding failure mode, Fig. 1. The available traction-separation model assumes initially linear elastic behavior followed by the initiation and evolution of damage. This model was suggested by Fernando (2010) depending on numerical validation using the experimental work of (Deng and Lee 2007). Also, Obaidat *et al.* (2010b)

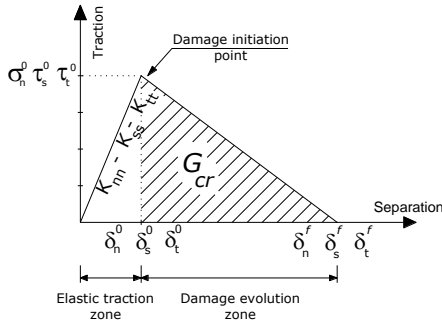


Fig. 1 Description of the traction-separation behavior, (ABAQUS)

used that model with values induced based on the experimental study of Guo *et al.* (2005).

Using surface-based cohesive behavior which is primarily intended for situations in which the interface thickness is negligibly small, which can be used to model the delamination at interfaces directly in terms of traction versus separation in the three local directions; in the normal and the two shear directions, respectively of the surface. It assumes that failure of the cohesive bond is characterized by progressive degradation of the cohesive stiffness, which is driven by a damage process, (ABAQUS). The interface thickness is considered negligibly small, and the initial stiffness  $K_{nn}$ ,  $K_{ss}$ , and  $K_{tt}$ , in the normal and two shear directions, respectively defined as Obaidat *et al.* (2010a) and Sakr *et al.* (2014) with expression in Eq. (1)

$$K_{nn} = \frac{1}{\frac{t_i}{E_i} + \frac{t_c}{E_c}}, \quad k_{ss} = k_{tt} = \frac{1}{\frac{t_i}{G_i} + \frac{t_c}{G_c}} \quad (1)$$

Where  $t_i$  is the resin thickness,  $t_c$  is the concrete thickness, and  $G_i$  and  $G_c$  are the shear modulus of resin and concrete, respectively, and  $E_i$  and  $E_c$  are the modulus of elasticity of the resin and concrete, respectively, (Obaidat *et al.* 2010b).

Damage initiation refers to the beginning of degradation of the cohesive response at a contact point. The process of degradation begins when the contact stresses and/or contact separations satisfy certain damage initiation criteria. Maximum stress criterion was used which assumes that, the initiation of damage occurred when the maximum contact stress ratio reaches a value of one as defined in Eq. (2)

$$\max \left\{ \frac{\sigma_n}{\sigma_n^0}, \frac{\tau_s}{\tau_s^0}, \frac{\tau_t}{\tau_t^0} \right\} = 1 \quad (2)$$

Where  $\sigma_n^0$ ,  $\tau_s^0$ , and  $\tau_t^0$  represent the peak values of the contact stress when the separation is either purely normal to the interface or purely in the first or the second shear direction respectively, and  $\sigma_n$  is the cohesive tensile stress and  $\tau_s$ , and  $\tau_t$  are the cohesive shear stress in the two perpendicular directions  $s$  and  $t$ .

From Fig. 1, it is obvious that the relationship between the traction stress and effective opening displacement is defined by the elastic stiffness,  $K_{nn}$ ,  $K_{ss}$ , and  $K_{tt}$ , the local strength of the material,  $\sigma_n^0$ ,  $\tau_s^0$ , and  $\tau_t^0$ , and the energy needed for opening the crack,  $G_{cr}$ , which is equal to the area under the traction-displacement curve. Interface damage evolution was expressed in terms of energy release. The

description of this model is available in (ABAQUS). The dependence of the fracture energy on the mode mix was defined based on the Benzeggagh and Kenane (1996) fracture criterion.

### 2.3 Elements and meshing

In this study, behavior of RC shear walls was investigated with three different micro models using (ABAQUS) package. The analysis included 2D model using plane stress element, 3D model using shell element, and 3D model using solid element. Moreover, the 2D model using shell element was extended to investigate the behavior of CFRP retrofitted RC shear walls. At 3D analysis using solid element, an 8-node 3-D solid element (**C3D8R**) is used for modeling the concrete and CFRP sheets to overcome the possible errors and to consider the cracks in tension. Then a 2-node linear 3-D truss (**T3D2**) element was used for the RFT. Using 3D shell element, a 4-node doubly curved thin or thick shell, reduced integration, hourglass control, finite membrane strains (**S4R**) was used for modeling the concrete and CFRP sheets. While a 2-node linear 3-D truss (**T3D2**) element was used for modeling the reinforcement steel. At 2D analysis using 2D plane stress element, a 4-node bilinear, reduced integration with hourglass control elements (**CPS4R**) was used for the concrete and CFRP sheets. For the reinforcement steel a 2-node linear 2-D truss (**T2D2**) element was used. A perfect bond between steel reinforcement and concrete was assumed.

### 3. Verification of the model with previous work

In order to validate the accuracy and applicability of non-linear FE model of RC shear wall strengthened with FRP composites under monotonic loading, experimental data was used from previous work by Altin *et al.* (2013). The experimental study focused on the behavior of bare and CFRP retrofitted RC shear walls with different bracing configurations. Altin *et al.* (2013) have presented experimental results on  $\frac{1}{2}$  scale five specimens with 1.5 aspect ratio walls. One of them was tested without any retrofitting as a reference specimen and the rest were retrofitted specimens with CFRP strips. All of the specimens were tested under cyclic lateral loading. The cross bracing retrofitting scheme was selected to perform the current study. The dimensions and reinforcement (RFT) details of the reference RC shear wall are shown in Fig. 2(a). The CFRP strips were symmetrically applied to both sides of the RC wall and were bonded to the surface using epoxy resin. The CFRP strips were anchored to the RC wall by fan type of anchorages. The detailed descriptions of applied CFRP configurations and the distances between the anchorages are given in Fig. 2(b).

#### 3.1 Material properties

In the experimental study, specimens with low compressive strength were constructed to represent the concrete strength of the existing old buildings. The average compressive strength  $\bar{\sigma}_c$  was in the experimental work to

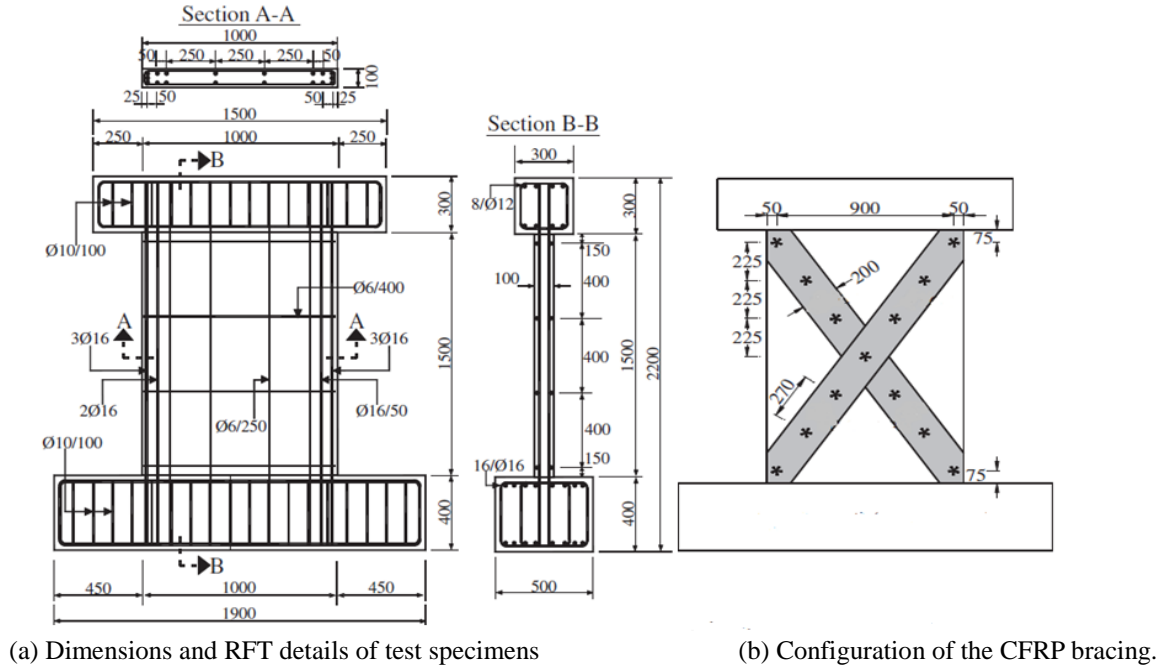


Fig. 2 The experimental specimen in the reference work of Altin *et al.* (2013)

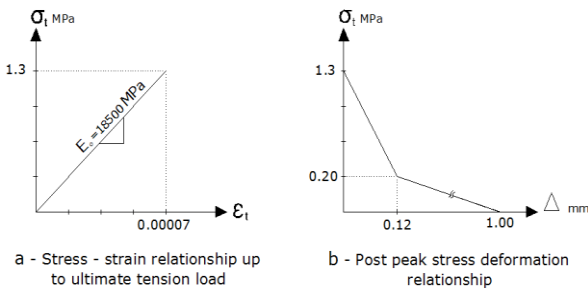


Fig. 3 Concrete behavior for uniaxial tension

15MPa.  $E_c$  and  $\sigma_{ct}$  were then calculated as shown in Fig. 3. Poisson’s ratio for concrete was assumed to be 0.20.

For the RFT steel, the elastic modulus,  $E_s$  and Poisson’s ratio used in the referenced experimental work was not provided, so the elastic modulus for the RFT steel was assumed to be 200 GPa and Poisson’s ratio to be 0.3. The yield strength,  $\sigma_y$  and the failure strength,  $\sigma_u$  used in the specimens are listed in Table 1.

According to Altin *et al.* (2013) the modulus of elasticity of the CFRP is 231 GPa and the tensile strength and ultimate tensile strain are 4100 MPa and 1.7%, respectively. The width of strip is 200 mm and its thickness was 0.12 mm was bonded to the surface using epoxy resin. The modulus of elasticity of the resin is 3.8 GPa and the tensile strength is 30 MPa. Modeling the CFRP anchor has been presented in this paper in section (4.3).

### 3.2 Adhesive layer properties

For 3D model using shell element or solid element, the adhesive layer was modeled using cohesive surface-to-surface interaction model. The values used for this study were  $t_i=1.5$  mm,  $t_c=25$  mm,  $G_i=0.665$  GPa, and  $G_c=10.8$  GPa, and for  $E_i=3.8$  GPa,  $E_c=18200$  MPa. The maximum

Table 1 Properties of reinforcements

Reinforcement diameter	Yield strength $\sigma_y$ (MPa)	Failure strength $\sigma_u$ (MPa)	Type
6	325	420	Plain
10	430	522	Deformed
12	428	515	Deformed
16	425	520	Deformed

shear stress,  $\tau_{max}$  was taken 1.5 MPa (Obaidat *et al.* 2010a). For the maximum normal stress, it was taken equal to the concrete tensile strength 1.27 MPa. For the fracture energy,  $G_{cr}$  in the two shear directions, previous researches have indicated values from 300 J/m<sup>2</sup> up to 1500 J/m<sup>2</sup>, Obaidat *et al.* (2010b). The cohesive model with fracture energy equal 900 J/m<sup>2</sup>, shown good an agreement with the experimental results. The value used for the fracture energy,  $G_{cr}$  in the normal direction equals 100 J/m<sup>2</sup> and for  $\eta = 1.45$ , Obaidat *et al.* (2010b).

For 2D model using shell element, the node-to-node interaction method using Cartesian elastic-plastic connector element was used. Cartesian connector element provided a connector between two nodes that allows independent behavior in two local Cartesian directions.

It is very important to notice that, in the experimental work the CFRP was installed on the both faces of the RC shear wall. So the stiffness, strength, fracture energies and also the CFRP sheet thickness values were multiplied by two, and then were installed on one surface.

### 3.3 Applied loads

In the experimental work, the base of the test specimen was anchored to the laboratory’s strong floor by high strength steel bolts. A steel stability frame was constructed around the test specimen to prevent out-of-plane

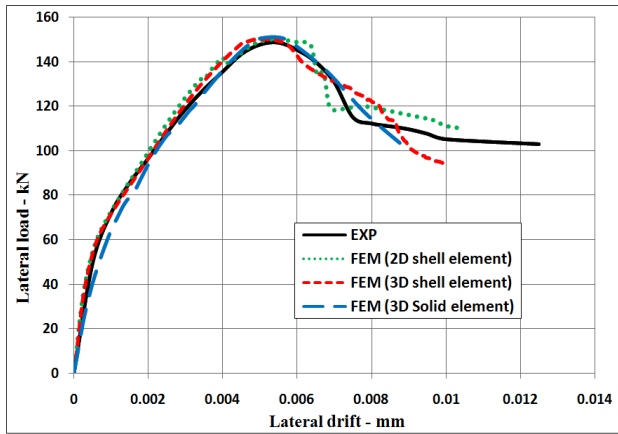


Fig. 4 Lateral load vs. lateral drift for bare RC shear wall

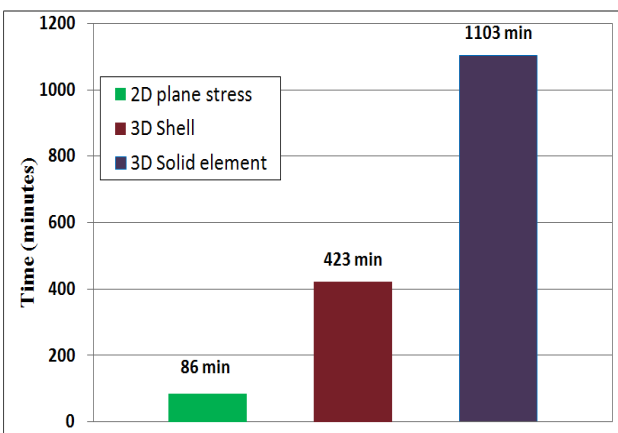


Fig. 5 CPU time in minutes for the different model types

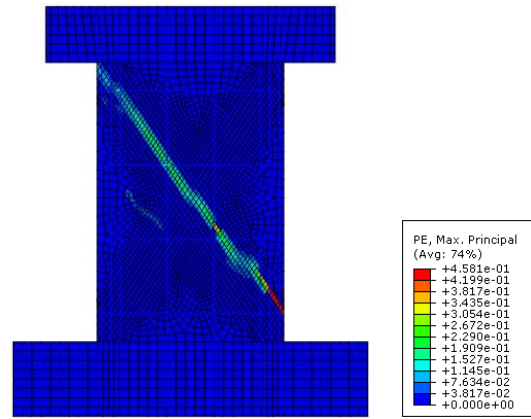
deformations. Specimens were tested under cyclic lateral loading. Each specimen was loaded laterally as a vertical cantilever with forces applied through the top beam. The lateral load was created by a hydraulic jack. Magnitudes of the force were measured by a load cell (500 kN compression -500 kN tension capacities). No axial load was applied to specimens. During the test, the top displacements and the lateral loads applied to specimen were monitored.

The envelopes of lateral load versus lateral drift displacement hysteretic curves for each specimen are given in the reference work of Altin *et al.* (2013). This can be used for verifying FE model under monotonic lateral load with the experimental work.

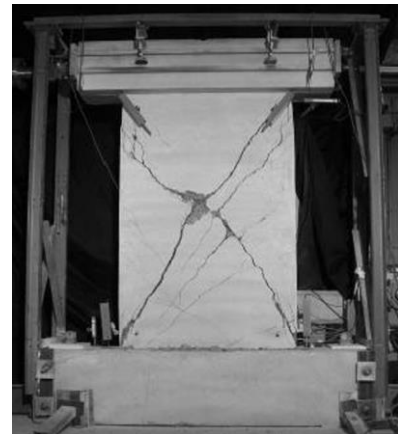
### 3.4 Comparison of experimental and finite element results

#### 3.4.1 Bare RC shear wall

The lateral load vs. lateral drift curves obtained for the bare RC shear wall from experimental and FE analysis are shown in Fig. 4. Also, Fig. 6(a)-(b) compare between the experimental and FE modes of failure of the bare RC shear wall. The mode of failure in FE is one diagonal concentrated shear cracks due to uni-direction monotonic lateral loading. While the specimen in experimental was tested under reversed cyclic lateral loading. The good agreement of the concentrated shear cracks in one diagonal



(a) Concrete plastic strain distribution for 2d plain stress model



(b) Damage pattern for bare RC shear wall (Altin *et al.* 2013)

Fig. 6 Mode of failure and crack survey

of the bare RC shear wall indicates that the constitutive models used for concrete and reinforcement can reasonably capture the mechanical behavior.

Fig. 5 shows a comparison of the central processing unit (CPU) time, the amount of processing time used of ABAQUS using (Intel Core i7-4500U) processor, of the proposed three models for the bare RC shear walls. It shows a great difference in the CPU time depending on the model type. The 2D plane stress model consumed about 20.3% of the 3D shell model CPU time and about 7.7% of the solid element model CPU time. Given the minor difference of the behavior observed between the three models and with reference to CPU time, it can be stated that, the 2D Plane stress element can be considered the most effective model among the three models.

#### 3.4.2 Cross braced CFRP strengthened RC shear wall

The lateral load vs. lateral drift curves obtained for the CFRP strengthened RC shear walls from experimental and FE analysis are shown in Fig. 7. Also, Fig. 8 demonstrates the yielding zones of the RFT of the CFRP strengthened RC shear wall. Fig. 9(a)-(b) compare between the experimental and FE modes of failure of the CFRP strengthened RC shear walls. Shear cracks were concentrated through the diagonal of the RC shear wall and after ultimate lateral load

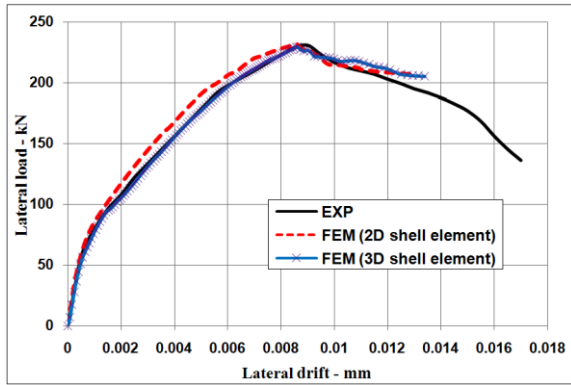


Fig. 7 Lateral load vs. lateral drift for the CFRP strengthened RC shear wall

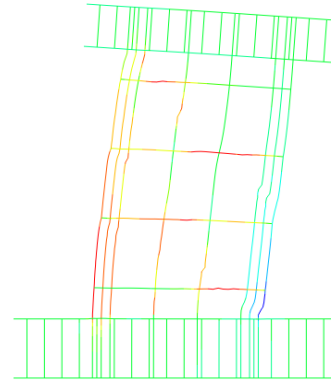
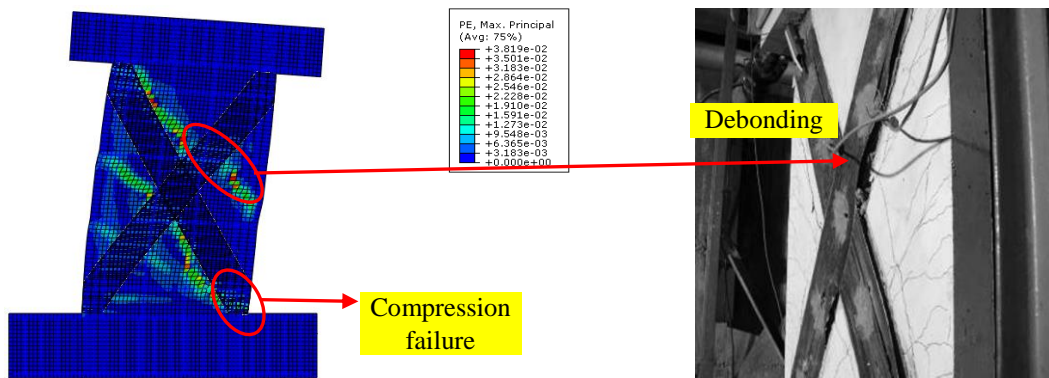


Fig. 8 Yielding stress zones in the RFT steel for 2d plain stress model



(a) Concrete plastic strain distribution for 2d plain stress model (b) Damage pattern for the CFRP strengthened RC shear wall (Altin *et al.* 2013)

Fig. 9 Mode of failure and crack survey

these cracks were widened due to separation of CFRP strips from the wall surface with increasing lateral load. The concrete was crushed at the bottom corner of the wall under the compressive stresses. The numerical simulations agree well with test results, indicating that the numerical method could accurately predict the behavior of RC shear walls strengthened with CFRP composites.

#### 4. Parametric study

To investigate some of the factors which could affect the transfer of shear stress at the bond layer under monotonic loading, nonlinear FE failure analysis of 2D shell elements have been developed using (ABAQUS) program. All RC shear walls have the same overall cross-sectional dimensions and internal longitudinal reinforcement as shown in Fig. 2(a). Four different parameters have been studied. These parameters are:

- Effect of the maximum shear stress,  $\tau_{max}$  and the fracture energy,  $G_{cr}$  for the cohesive bond between CFRP and wall.
- Effect of partial bonding of the CFRP sheets to the RC shear wall surface.
- A proposed CFRP anchor location, based on the transfer of shear stress at the bond layer, to delay the debonding.

- Effect of using different bracing configurations of CFRP strips with same area on the shear capacity of strengthened RC shear walls.

##### 4.1 Effect of shear stress, $\tau_{max}$ and fracture energy, $G_{cr}$

To investigate to what extent  $\tau_{max}$  affects the results, five cohesive bond models were tested with  $F_{cu}=30$  MPa and  $\tau_{max}=0.5$  MPa, 1.5 MPa, 2.25 MPa, 3 MPa, and full bond, respectively. Where  $G_{cr}$  was assumed a constant value equals  $900 \text{ J/m}^2$ , and the results are shown in Fig. 10.

For fracture energy,  $G_{cr}$ , previous researches have indicated values from  $300 \text{ J/m}^2$  up to  $1500 \text{ J/m}^2$  (Obaidat *et al.* 2010b). To investigate to what extent  $G_{cr}$  affects the results five cohesive bond models with  $F_{cu}=30$  MPa were performed for  $G_{cr}=300 \text{ J/m}^2$ ,  $700 \text{ J/m}^2$ ,  $900 \text{ J/m}^2$ ,  $1200 \text{ J/m}^2$  and full bond, respectively taking  $\tau_{max}=1.5$  MPa as a suitable value and the results are shown in Fig. 11. The results showed that, increasing the capacity of shear stress,  $\tau_{max}$  at a constant value of fracture energy increase slightly the ductility of the RC shear wall strengthened by CFRP. While increasing the fracture energy value at a constant value of shear stress,  $\tau_{max}$  leads clearly to delay the occurrence of debonding, and thus increases the ultimate load, the corresponding lateral drift and the ductility of the RC shear wall strengthened by CFRP.

The perfect bond model overestimates the stiffness at

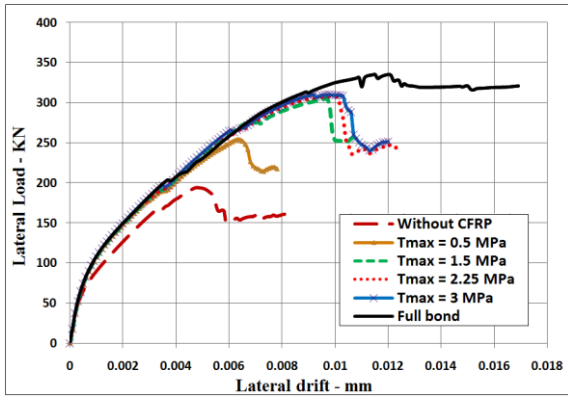


Fig. 10 Lateral load vs. lateral drift for different interfacial shear stresses,  $\tau_{max}$  at  $F_{cu}=30 \text{ N/mm}^2$ ,  $G_{cr}=900 \text{ J/m}^2$

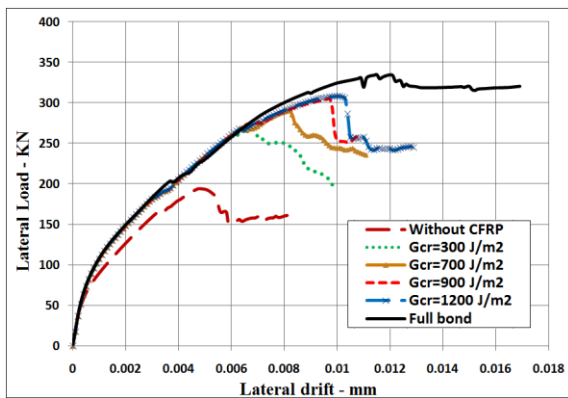


Fig. 11 Lateral load vs. lateral drift for different fracture energy,  $G_{cr}$  at  $F_{cu}=30 \text{ N/mm}^2$ ,  $\tau_{max}=1.5 \text{ MPa}$

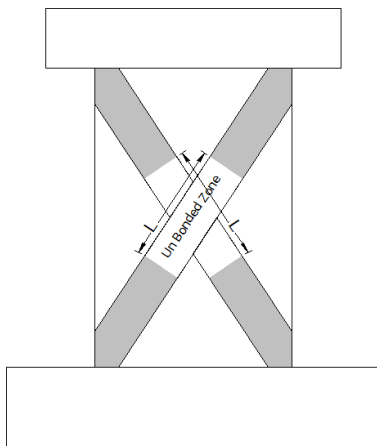
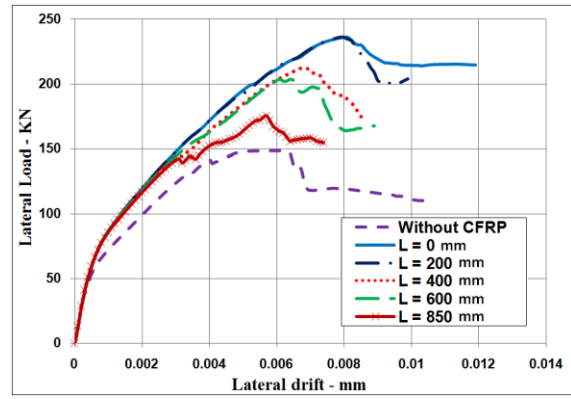


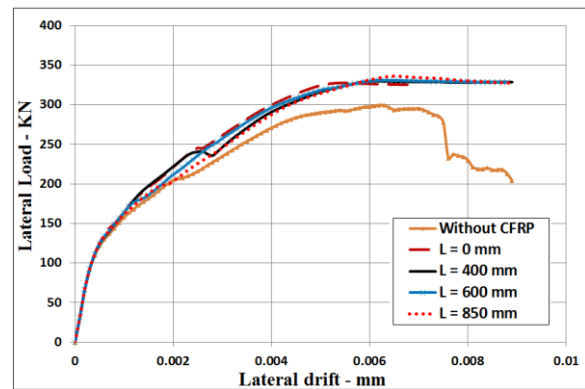
Fig. 12 Unbonded length “L”

the intermediate loading stage and the ultimate load and also another mode of failure occurs, where the cohesive model is able to represent more accurately the bond behavior between CFRP and concrete. diagonal length and increasing that bonding length does not lead to an increase in the ultimate behavior of the strengthened RC shear wall.

#### 4.2 Effect of partial bonding of the CFRP sheets to the RC shear wall surface



(a)  $F_{cu}=15.5 \text{ N/mm}^2$ ,  $t_w=100 \text{ mm}$



(b)  $F_{cu}=40 \text{ N/mm}^2$ ,  $t_w=200 \text{ mm}$

Fig. 13 Lateral load vs. lateral drift for partial bonding of the CFRP sheet with unbonded length “L”

In this study, the cross bracing CFRP strengthened RC shear wall was reanalyzed, but in the presence of a new variable which is the unbonded length (L) as shown in Fig. 12. Two CFRP strengthened RC shear walls with different values of concrete strength and wall thickness equal ( $F_{cu}=15.5 \text{ N/mm}^2$ ,  $t_w=100 \text{ mm}$ ) and ( $F_{cu}=40 \text{ N/mm}^2$ ,  $t_w=200 \text{ mm}$ ), respectively were analyzed.  $\tau_{max}=1.5 \text{ MPa}$ ,  $G_{cr}=900 \text{ J/m}^2$  were utilized to represent the interface between concrete and CFRP. The unbonded length varied as 200 mm, 400 mm, 600 mm and 850 mm. The lateral load vs. lateral drift curves obtained for the two CFRP strengthened RC shear walls with different unbonded length (L) are shown in Fig. 13 (a)-(b)

Fig. 13(a) shows that, the load capacity decrease by increasing the unbonded length (L). While Fig. 13(b) shows a slight difference in behavior of the partial bonding RC shear walls strengthened by CFRP compared to the totally bonding one. This figure shows a ductile flexural behavior and at the base of the wall the plastic hinge has been developed. From these results, when the mode of failure of the bare RC shear wall is shear failure, the partial bonding has a great effect on the strengthened RC shear wall behavior. On the other hand, when the mode of failure is flexure the effect of the partial bonding is very small. It is clear at RC shear wall with ( $F_{cu}=40 \text{ N/mm}^2$ ,  $t_w=200 \text{ mm}$ ), the minimum bonding length of the CFRP sheet on the RC shear wall panel to get the same behavior of the totally bonded model was about 50% of the RC shear wall panel diagonal length and increasing that bonding length does not

lead to an increase in the ultimate behavior of the strengthened RC shear wall.

### 4.3 A proposed CFRP anchor location

The tension stresses that can be developed in CFRP sheets bonded to concrete represent only a fraction of the rupture strength of the sheet due to the premature failure by debonding. In order to make CFRP strengthening applications more efficient, a ways to anchor the sheets so that failure by debonding was precluded. Various ways of anchoring the CFRP sheets to concrete have been investigated by researchers, including the use of transverse sheets or straps, using mechanical anchors, wrapping the end of sheets in rods embedded in grooves formed into the concrete, or using CFRP anchors (Brena and McGuirk, 2013).

In order to model the mechanical representation of the CFRP anchor response, Brena and McGuirk (2013) proposed force-deformation relationship for modeling the CFRP anchors for shear rupture failure mode. They proposed two types of CFRP anchors, the first type was 13 mm anchor diameter with 51 mm splay diameter, where the second type was 19 mm anchor diameter and 102 splay diameter as shown in Fig. 14 and Table 2. The tension behavior of the anchor is the axial tension strength of the CFRP sheet used to make the anchor.

In order to convert this force-displacement behavior to a traction separation behavior, the elastic traction separation behavior was defined, and then the initiation of damage, and finally damage evolution part as shown in Fig. 15. For damage evolution, the maximum displacement criteria was used instead of the maximum dissipated energy where  $\delta_{max}=1.78$  mm. These data are illustrated in Table 2.

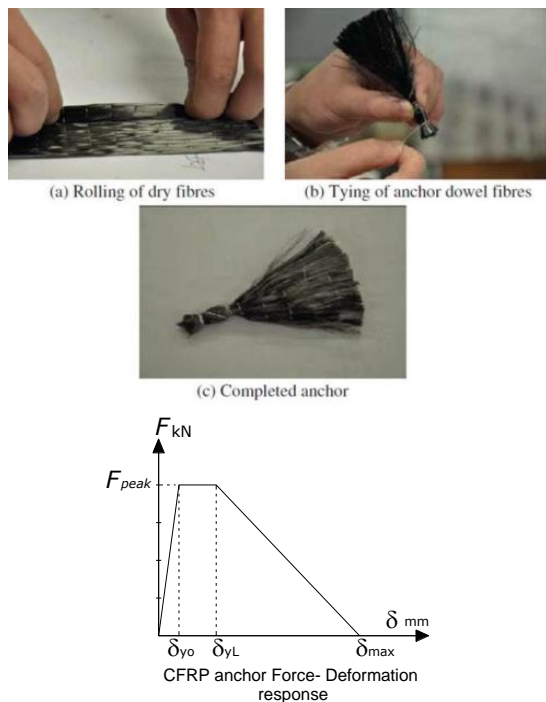


Fig. 14 Proposed force-deformation relationship for the modeling of the CFRP anchors (Brena and McGuirk 2013)

Fig. 17(a)-(b) show a complete convergence between the behavior of the reference model SW-1 without anchors and SW-2 model with one row of anchors. This indicates that, using one row of seven anchors at middle of each one of the two diagonal CFRP strips will not lead to an increase in the ultimate behavior of the strengthened RC shear wall.

Also, as illustrated in Fig. 17(a)-(b), the behavior of SW-3 was improved comparing with the case of without anchors SW-1. This indicates that, when the mode of failure of the bare RC shear wall is shear or flexure, using two 13 mm anchors near each end of CFRP strips with distances as shown in Fig. 16, delay the end debonding and increase the ductility for CFRP strengthened RC shear walls which is very useful in case of seismic event. The failure mode for CFRP strengthened RC shear walls with  $F_{cu}=15$  N/mm<sup>2</sup> is debonding as shown in Fig. 18.

### 4.4 Different bracing configurations of CFRP strips with same area

In this section, to show the effect of the CFRP strips configuration on the load-capacity of CFRP strengthened RC shear walls, four RC shear walls strengthened with same area of CFRP strips but with different configurations, SW-4, SW-5, SW-6 and SW-7, were modeled, as shown in Fig. 19. These RC shear walls were analyzed in two cases, first one with concrete strength,  $F_{cu}=15$  N/mm<sup>2</sup> and the other case with  $F_{cu}=40$  N/mm<sup>2</sup>. The thickness of walls,  $t_w=100$  mm,  $\tau_{max}=1.5$  MPa,  $G_{cr}=900$  J/m<sup>2</sup> were used to represent the interface between concrete and CFRP.

Fig. 20(a) shows when the mode of failure of the bare RC shear wall is shear failure, the best performance to improve lateral strength and ductility of RC shear walls has

Table 2 Response parameters for CFRP anchor modeling (Brena and McGuirk 2013)

	Small CFRP anchor $d_a=13$ mm, $d_s=51$ mm	Large CFRP anchor $d_a=19$ mm, $d_s=102$ mm
$F_{peak}$ (kN)	17.8	22.7
$\delta_{yo}$ (mm)	0.18	0.25
$\delta_{yL}$ (mm)	0.51	0.64
$\delta_{max}$ (mm)	1.78	1.78

\* $d_a$  is the anchor diameter, and  $d_s$  is the splay diameter

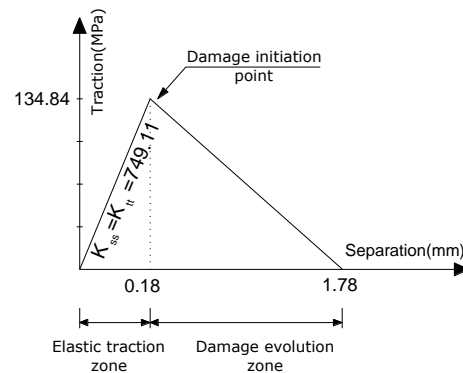


Fig. 15 Traction separation behavior of the CFRP 13mm anchor

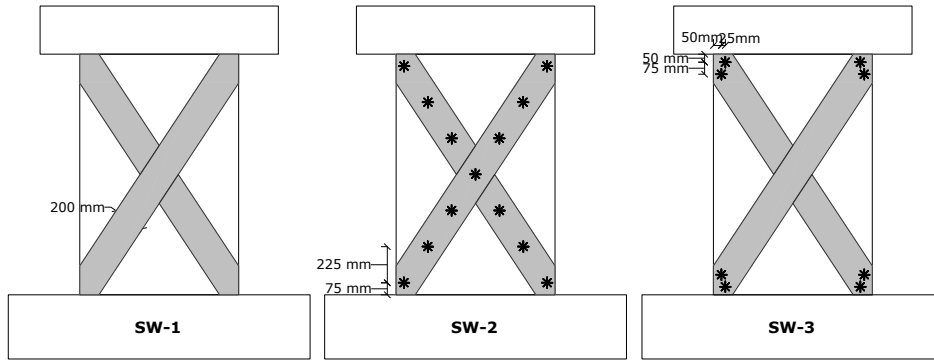
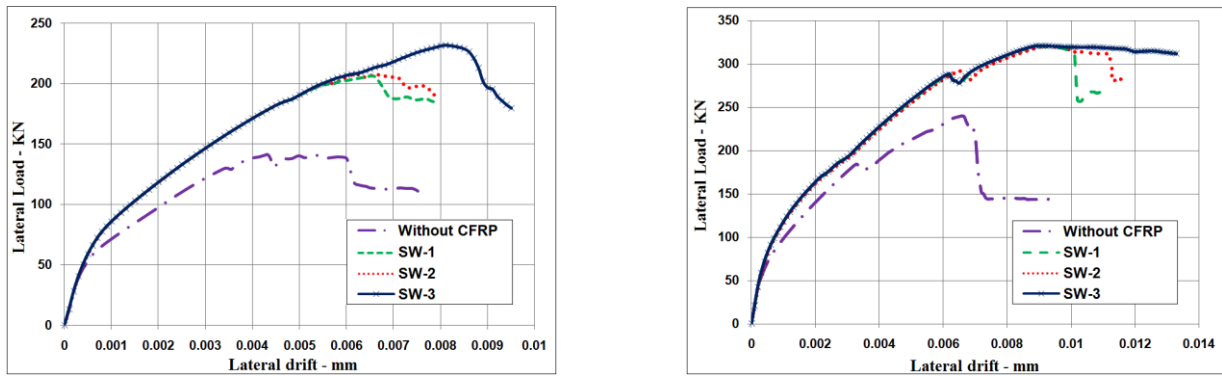


Fig. 16 The arrangements of CFRP anchors and the distances between them



(a)  $F_{cu}=15 \text{ N/mm}^2$ ,  $\tau_{max}=0.5 \text{ MPa}$ ,  $G_{cr}=300 \text{ J/mm}^2$ ,  $t_w=100 \text{ mm}$  (b)  $F_{cu}=40 \text{ N/mm}^2$ ,  $\tau_{max}=1.5 \text{ MPa}$ ,  $G_{cr}=900 \text{ J/mm}^2$ ,  $t_w=100 \text{ mm}$

Fig. 17 Lateral load vs. lateral drift for different anchor locations for CFRP strengthened RC shear walls

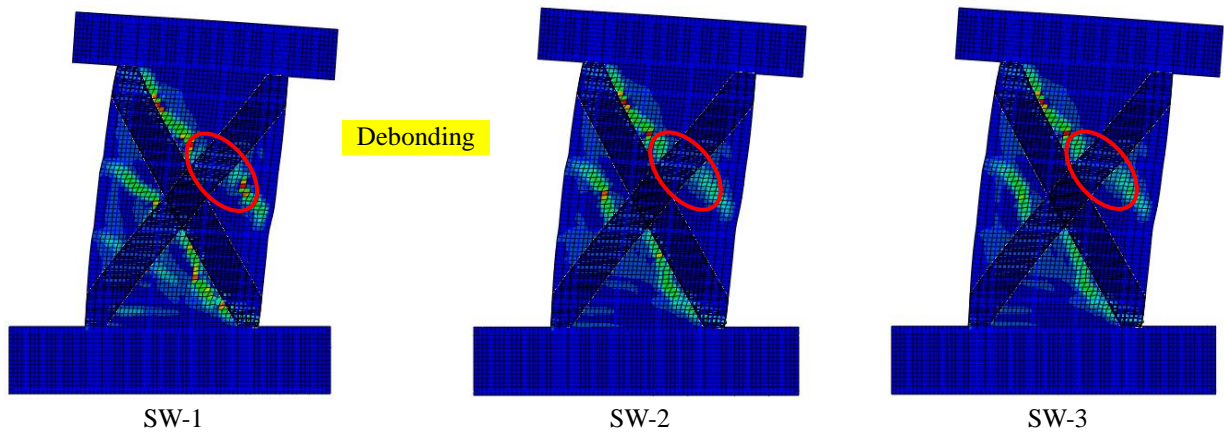


Fig. 18 Concrete plastic strain distribution at ultimate load for SW-1, SW-2 and SW-3 ( $F_{cu}=15 \text{ N/mm}^2$ ,  $\tau_{max}=0.5 \text{ MPa}$ ,  $G_{cr}=300 \text{ J/mm}^2$ )

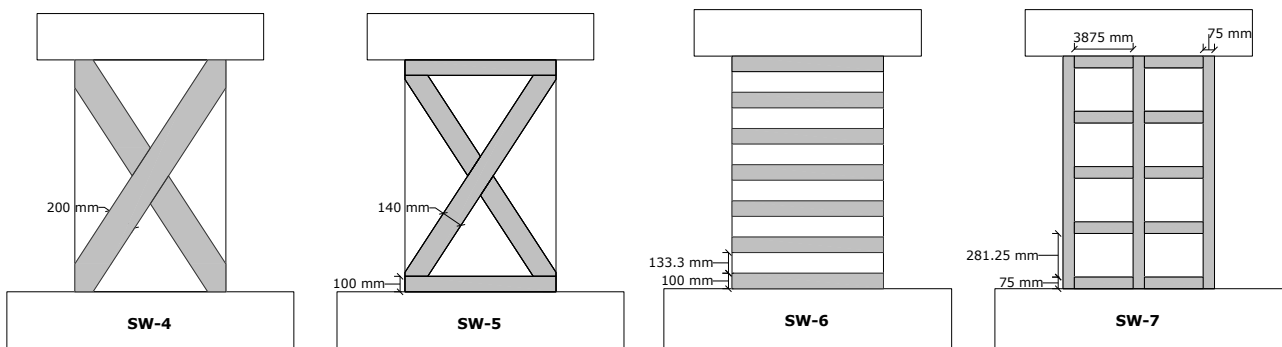


Fig. 19 Different bracing configurations of CFRP strips with same area

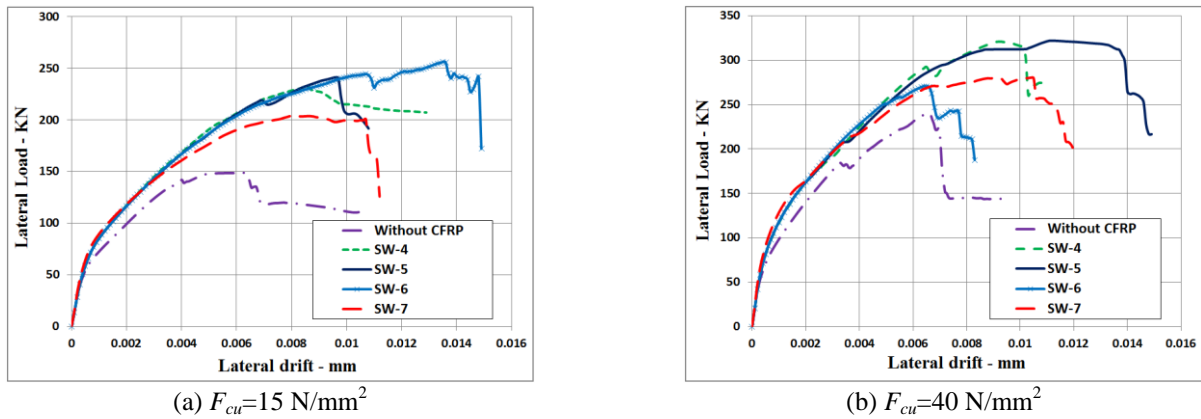


Fig. 20 Lateral load vs. lateral drift for different bracing configurations of CFRP strips with same area

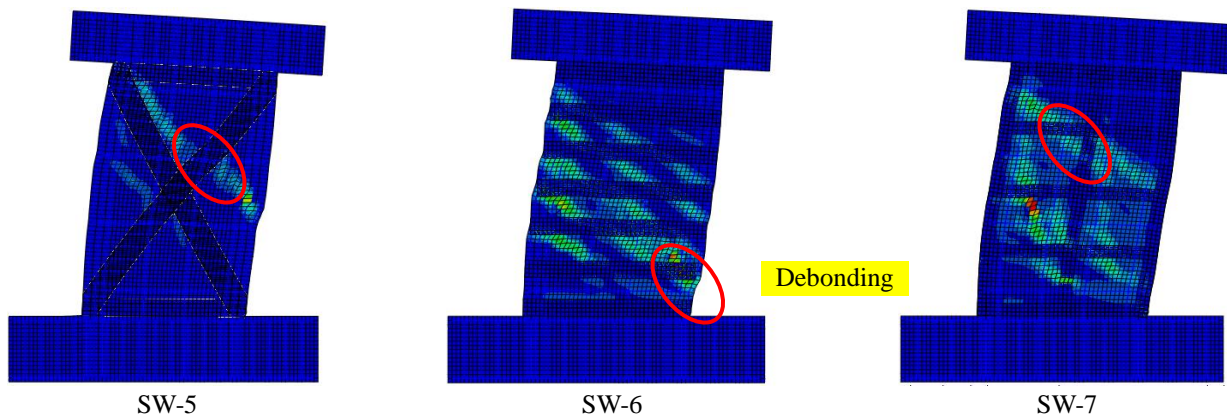


Fig. 21 Concrete plastic strain distribution for SW-5, SW-6 and SW-7 at ultimate load ( $F_{cu}=15 \text{ N/mm}^2$ )

been obtained by strengthening with lateral strips, SW-6. The failure mode for strengthened RC shear walls is debonding as shown in Fig. 21. The concrete plastic strains for SW-4 are similar to that of SW-1.

The mode of failure of the bare RC shear wall with  $F_{cu}=40 \text{ N/mm}^2$  is flexure. Fig. 20(b) shows, depending on utilizing same area for CFRP sheets, there is an increasing in the ultimate load capacity of bare RC shear wall for specimens SW-4, SW-5, SW-6 and SW-7 with ratios 33.7%, 34.15%, 12.77% and 16.63%, respectively. SW-4 and SW-5 strengthened the flexural behavior by the vertical component of the diagonal CFRP sheet.

In addition, for SW-5, the horizontal CFRP sheet anchored the ends of the diagonal CFRP sheets to improve end bonding. The best performance for the improvement of lateral shear strength and ductility of RC shear walls has been obtained by strengthening with cross strips and lateral strips combination, SW-5. The worst performance, among the aforementioned strengthening configurations, for the overall behavior of the CFRP strengthened RC shear wall has been obtained by strengthening with lateral strips, SW-6. This is because the lower CFRP sheet at SW-6 only relocated the flexural crack above this sheet and there is no boundary vertical CFRP sheet. SW-7 strengthened the flexural failure by the boundary vertical CFRP sheet but with relatively small area.

By increasing the width of the horizontal and diagonal CFRP sheets to 200 mm, the overall behavior of the CFRP

strengthened RC shear wall was improved. The ultimate load capacity was increased by 41.44% of the bare RC shear wall. Also, in the case of utilizing an anchorage device for the horizontal CFRP sheet at the lower part of wall extended to the base, the specimen strength and energy dissipating capacity were improved significantly. The ultimate load capacity was increased by 59.12% of the bare RC shear wall.

## 5. Conclusions

This paper has been concerned with the accurate prediction of debonding failures in RC shear walls strengthened by CFRP strips using the FE method. A FE approach has been presented, in which the cohesive zone model is employed to represent nonlinear fracture including interfacial debonding between concrete and FRP. Using the proposed FE approach, the behavior of CFRP-strengthened RC shear walls is examined, indicating that:

- The perfect bond model overestimates the stiffness at the intermediate loading stage and the ultimate load and also another mode of failure occurs, where the cohesive model is able to represent more accurately the bond behavior between CFRP and concrete.
- Utilizing adhesive layer with higher fracture energy value leads clearly to increase the ultimate load and the dissipated energy in addition to increase of the structure

ductility.

- When the mode of failure of bare RC shear wall is shear, the partial bonding of the CFRP sheet to the RC shear wall surface has a big effect of the overall behavior of the CFRP strengthened RC shear wall. But when the mode of failure of RC shear wall is flexure, the partial bonding has a little effect on this behavior. The results of the current solved examples showed; to get the highest efficiency of the CFRP strengthened RC shear wall, bonding only about 50% of the diagonal length is sufficient from each end to get the same behavior as the totally bonded sheet.
- By identifying the position of the maximum contact shear stress, the perfect place of CFRP anchors can be located. Modeling of the CFRP anchor must be capable of representing the mode of failure of the real anchor. Using two anchors near each end of diagonal CFRP strips delay the end debonding and increase the ductility for RC shear walls.
- The strip configurations were effective on the behavior of CFRP strengthened RC shear wall. When the mode of failure of bare RC shear wall is shear, the best performance for improvement of lateral strength and ductility of RC shear walls has been obtained by strengthening with lateral strips, SW-6. But when the mode of failure is flexure, the best performance has been obtained by strengthening with cross strips and lateral strips combination, SW-5.

## References

- Abaqus, "Abaqus/CAE User's Manual", Dassault Systemes Simulia Corp., Providence, RI, USA.
- Aci-318 (1999), Building code requirements for structural concrete and commentary. American Concrete Institute, Detroit (MI), USA.
- Alsayed, S.H., Almusallam, T.H., Ibrahim, S.M., Al-Hazmi, N.M., Al-Salloum, Y.A. and Abbas, H. (2014), "Experimental and numerical investigation for compression response of CFRP strengthened shape modified wall-like RC column", *Constr. Build. Mater.*, **63**, 72-80.
- Altin, S., Anil, O., Koprman, Y. and Kara, M.E. (2013), "Hysteretic behavior of RC shear walls strengthened with CFRP strips", *Compos. Part B: Eng.*, **44**(1), 321-329.
- Antoniades, K.K., Salonikios, T.N. and Kappos, A.J. (2007), "Evaluation of hysteretic response and strength of repaired R/C walls strengthened with FRPs", *Eng. Struct.*, **29**(9), 2158-2171.
- Behfarnia, K. and Sayah, A.R. (2012), "FRP strengthening of shear walls with openings", *Asian J. Civil Eng. (Build. Hous.)*, **13**(5), 691-704.
- Benzeggagh, M.L. and Kenane, M. (1996), "Measurement of mixed-mode delamination fracture toughness of unidirectional glass/epoxy composites with mixedmode bending apparatus", *Compos. Sci. Technol.*, **56**(4), 439-449.
- Brena, S.F. and Mcguirk, G.N. (2013), "Advances on the behavior characterization of FRP-anchored Carbon Fiber-Reinforced Polymer (CFRP) sheets used to strengthen concrete elements", *Int. J. Concrete Struct. Mater.*, **7**(1), 3-16.
- Christian, C., Kolluru, V.S., Marco, S. and Claudio, M. (2012), "Experimental determination of FRP-concrete cohesive interface properties under fatigue loading", *Compos. Struct.*, **94**, 1288-1296.
- Cruz, C., Lau, D.T. and Sherwood, E. (2012), "Testing and anchor system performance of RC shear walls repaired and strengthened with externally-bonded FRP sheets", *15th World Conference of Earthquake Engineering*, Lisbon, Portugal, September.
- Dan., D. (2012), "Experimental tests on seismically damaged composite steel concrete walls retrofitted with CFRP composites", *Eng. Struct.*, **45**, 338-348.
- Deng, J. and Lee, M.M.K. (2007), "Behaviour under static loading of metallic beams reinforced with a bonded CFRP plate", *Compos. Struct.*, **78**(2), 232-242.
- El-Sokkary, H. and Galal, K. (2013), "Seismic behavior of RC shear walls strengthened with fiber-reinforced polymer", *J. Compos. Constr.*, **10**, 603-613.
- Fernando, N.D. (2010), "Bond behaviour and debonding failures in CFRP-strengthened steel members", PhD Thesis, The Hong Kong Polytechnic University, Hong Kong, China.
- Guo, Z.G., Cao, S.Y., Sun, W.M. and Lin, X.Y. (2005), "Experimental study on bond stress-slip behaviour between FRP sheets and concrete", *FRP in Construction, Proceedings of the International Symposium on Bond Behaviour of FRP in Structures*, 77-84.
- Hu, H. and Schnobrich, W. (1989), "Constitutive modelling of concrete by using non associated plasticity", *J. Mater. Civil Eng.*, ASCE, **1**(4), 199-216.
- Li, Z.J., Balendra, T., Tan, K.H., Li, Z.J. and Kong, K.H. (2005), "Finite element modeling of cyclic behavior of shear wall structure retrofitted using GFRP", *Special Publication*, **230**, 1305-1324.
- Mohammed, B.S., Ean, L.W. and Malek, M.A. (2013), "One way RC wall panels with openings strengthened with CFRP", *Constr. Build. Mater.*, **40**, 575-583.
- Mostofinejad, D. and Anaei, M.M. (2012), "Effect of confining of boundary elements of slender RC shear wall by FRP composites and stirrups", *Eng. Struct.*, **41**, 1-13.
- Obaidat, Y.T., Heyden, S. and Dahlblom, O. (2010a), "The effect of CFRP and CFRP/concrete interface models when modelling retrofitted RC beams with FEM", *Compos. Struct.*, **92**(6), 1391-1398.
- Obaidat, Y.T., Heyden, S., Dahlblom, O., Farsakh, G.A. and Yahia, A.J. (2010b), "Retrofitting of reinforced concrete beams using composite laminates", *Constr. Build. Mater.*, **25**(2), 591-597.
- Qazi, S., Michel, L. and Ferrier, E. (2013), "Mechanical behaviour of slender rc wall under seismic loading strengthened with external bonded cfrp", *Eur. J. Environ. Civil Eng.*, **17**(6), 496-506.
- Qazi, S., Michel, L. and Ferrier, E. (2015), "Impact of CFRP partial bonding on the behaviour of short reinforced concrete wall under monotonic lateral loading", *Compos. Struct.*, **128**, 251-259.
- Saenz, L.P. (1964), "Discussion of 'Equation for the stress-strain curve of concrete' by Desayi P, Krishnan S", *ACI J.*, **61**(6), 1229-1235.
- Sakr, M.A., Khalifa, T.M. and Mansour, W.N. (2014), "External strengthening of RC continuous beams using FRP plates: finite element model", *Proceedings of the Second International Conference on Advances In Civil, Structural and Mechanical Engineering-CSM*, Birmingham, England.
- Zhou, H., Attard, T.L., Zhao, B., Yu, J., Lu, W. and Tong, L. (2013), "Experimental study of retrofitted reinforced concrete shear wall and concrete-encased steel girders using a new CarbonFlex composite for damage stabilization", *Eng. Fail. Anal.*, **35**, 219-233.